

Article

# Structural Diagenesis in Carbonate Rocks as Identified in Fault Damage Zones in the Northern Tarim Basin, NW China

Guanghui Wu <sup>1,2,\*</sup>, En Xie <sup>3</sup>, Yunfeng Zhang <sup>1</sup>, Hairuo Qing <sup>2</sup>, Xinsheng Luo <sup>3</sup> and Chong Sun <sup>3</sup>

<sup>1</sup> School of Geoscience and Technology, Southwest Petroleum University, Chengdu 610500, China; zhyf@swpu.edu.cn

<sup>2</sup> Department of Geology, University of Regina, Regina, SK S4S 0A2, Canada; Hairuo.Qing@uregina.ca

<sup>3</sup> PetroChina Tarim Oilfield Company, Korla 841000, China; xieen-tlm@petrochina.com.cn (E.X.); luoxs-tlm@petrochina.com.cn (X.L.); sunchong-tlm@petrochina.com.cn (C.S.)

\* Correspondence: wugh@swpu.edu.cn

Received: 5 May 2019; Accepted: 22 May 2019; Published: 13 June 2019



**Abstract:** The identification of structural diagenesis and the reconstruction of diagenetic paragenesis in fault damage zones is important for understanding fault mechanisms and fluid flow in the subsurface. Based on the examination of core and sample thin section data, we deciphered the diagenetic parasequence and their fault controls for Ordovician carbonates in the northern Tarim intracratonic basin in NW China (Halahatang area). In contrast to the uniform nature of diagenesis observed in country rocks, there is a relatively complicated style of compaction and pressure solution, multiple fracturing, and cementation and dissolution history along the carbonate fault damage zones. The relative paragenetic sequence of the structure related diagenesis suggests three cycles of fracture activities, following varied fracture enlargement and dissolution, and progressively weaker calcite cementation. These processes of structure related diagenesis are constrained to the fault damage zones, and their variation is affected by the fault activities. The results of this study suggest that the carbonate reservoir and productivity could be impacted by the structure related diagenesis locally along the fault damage zones.

**Keywords:** fault damage zone; carbonate; fracture; structural diagenesis; diagenetic sequence

## 1. Introduction

Brittle deformation (e.g., faulting) in the upper crust is a common phenomenon that can strongly influence any subsequent geological processes and indeed the hydraulic properties of the rocks affected by this type of deformation [1–3]. The generally complicated deformation structures, typical of large faults [1–6], may impart a complex diagenesis to these faulted zones [7–9]. For example, structures related to diagenesis can be pervasive and may alter mineralization pathways and cementation in a fault zone, especially in the case of carbonate rocks [8–10]. While the structure and microstructure of fault zones have been widely studied to better understand the process of faulting, by contrast, the diagenesis of and its integration with fault processes have been mostly neglected [1,2,9]. Structural diagenesis is the study of the relationships between deformation or deformational structures and chemical changes to sediments [9]. Whereas fault architecture and process can constrain the diagenesis along a fault zone, diagenetic processes can significantly influence the fault architecture, rock properties and mechanisms of brittle deformation leading to fracture or faulting [9–15]. Studies on the integration of fault process and structural diagenesis are helpful to understand not only the mechanisms of faulting, but also petrophysical properties and fluid flow along fault zones, promoting efforts in multidisciplinary studies of structure, reservoir characterization and diagenesis [9,16–22]. However, the fault elements and

diagenesis and their interaction are demonstrably complicated and varied in fault zones, particularly in the presence of multi-stage structural and diagenetic processes [15,19,23,24].

In this paper, we present data from and discuss a carbonate fault system with three distinct phases of fault activity in the intracratonic Tarim Basin, China. Geological rock cores and thin sections were studied and used to determine the fault-related diagenesis of the carbonate “damage zones”. Moreover, we examine the fracture cross-cutting and abutting relationships and orientations of veins to understand the parasequence of the structural diagenesis. In addition, we discuss the influences of fault activities on the carbonate diagenesis in the deep subsurface.

## 2. Geological Setting

The Tarim Basin is the largest petroliferous basin in NW China, with an area of 560,000 km<sup>2</sup> [25] (Figure 1a). It has an Archean-Early Neoproterozoic crystalline basement that is covered by thick sequence of late Neoproterozoic-Quaternary sedimentary strata with multi-stage sedimentary-tectonic evolution (Figure 1b) [25]. Key events include supercontinent breakup in the late Neoproterozoic, the opening and closure of Tethys in the Palaeozoic and the Mesozoic, and the Indo-Asian collision during the Cenozoic [25–27]. The Tarim Basin developed from the Cenozoic foreland basin and the Palaeozoic-Mesozoic intracratonic basin [25], following multi-phase tectonic movements, which involved various faults [25,27–30], developed in the intracratonic basin.

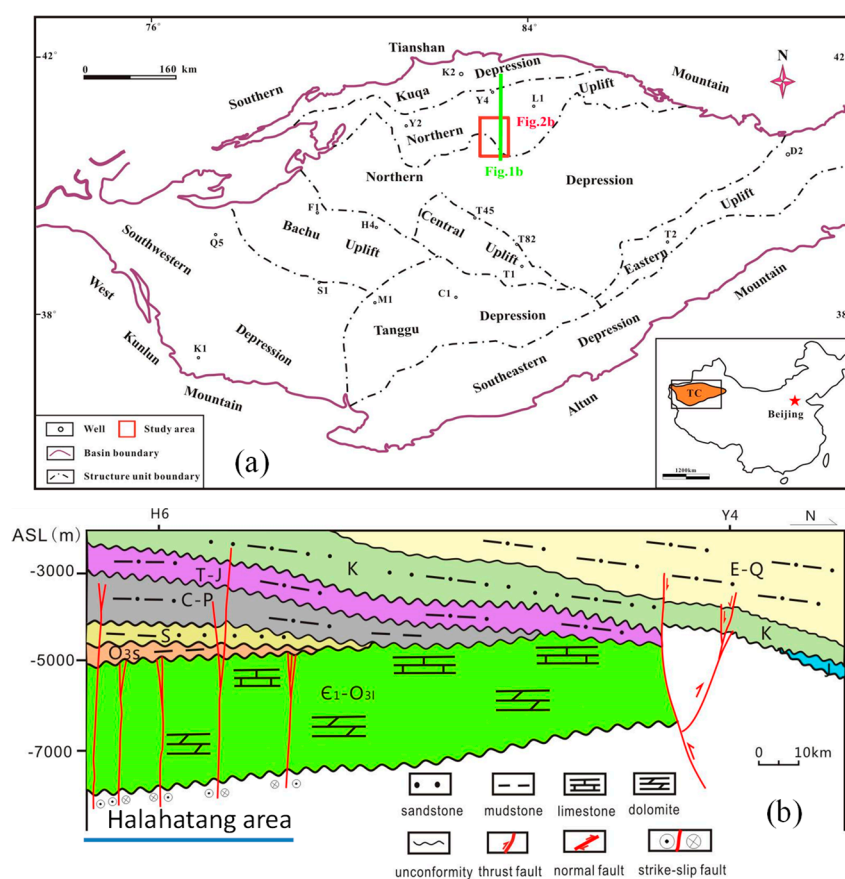


**Figure 1.** (a) The tectonic division of the Tarim Basin (the lower right inset map shows its location in China) (after [30]); (b) Geological profile across the study area (the upper strata of ~3000 m Cretaceous-Quaternary are omitted in the cross-section; modified from [30]). e: Cambrian; O<sub>31</sub>: Upper Ordovician Lianglitage Formation; O<sub>3s</sub>: Upper Ordovician Samgtamu Formation; S: Silurian; C-P: Carboniferous-Permian; T: Triassic; J: Jurassic; K: Cretaceous; E-Q: Eocene-Quaternary.

The Halahatang area investigated in this study, covering about 8000 km<sup>2</sup>, is located in the southern slope of the Northern Uplift, Tarim Basin (Figure 1a). At this site, the Phanerozoic strata are relatively complete, consisting of Cambrian–Ordovician carbonates, with a Silurian to Cretaceous sequence containing multiple unconformities, and a Cenozoic sequence representing rapid subsidence [25,29] (Figures 1b, 2a and 3a). Regional structural interpretation and fault mapping reveals a network of conjugate strike-slip fault systems that developed in the Cambrian–Ordovician, followed by some reactivation, in Silurian–Permian and Mesozoic–Eocene times by the process of faulting inheritance, with multi-layer flower structures (Figure 2) [29,30]. Many faults terminate at the top of the Upper Ordovician carbonate rocks; these generally show positive flower structures in Lower Palaeozoic strata, which resulted in horst blocks in the overlapping zones (Figure 2a) [29]. Fault zones in the Ordovician carbonates are up to 50–70 km in length (Figure 2b), but the vertical throw along a fault zone is generally in a range of 20–80 m [30].

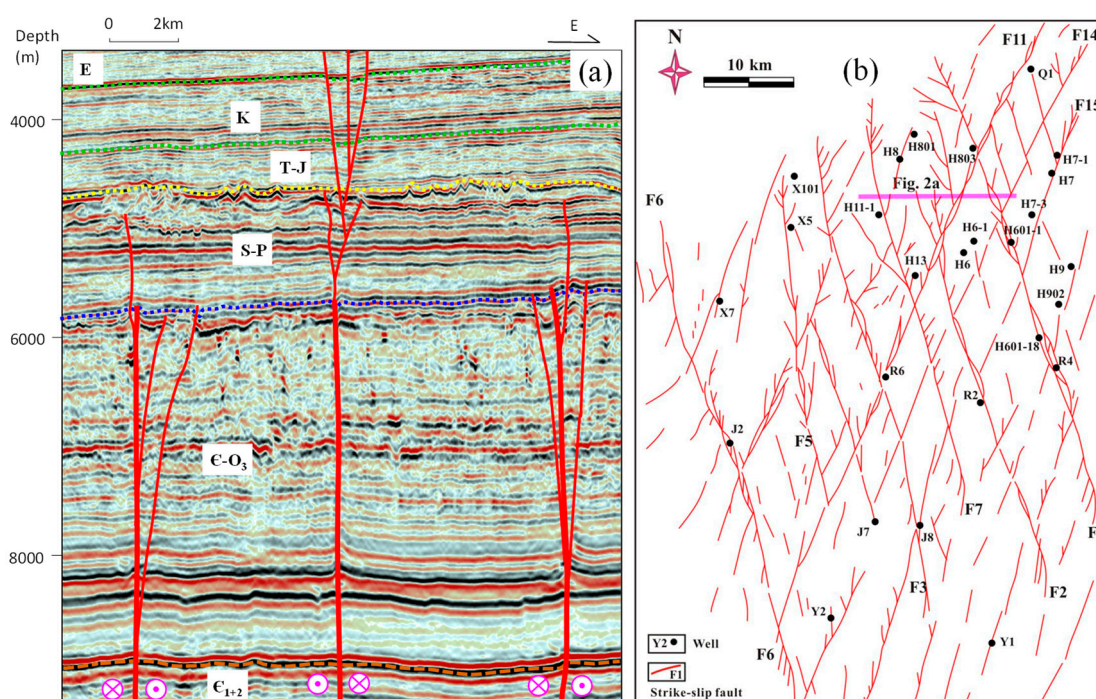


**Figure 2.** (a) Typical seismic sections showing the strike-slip faults (the strata symbols are same with Figure 1), and (b) the map view of the strike-slip fault system affecting the Ordovician carbonate sequence (~6500–7500 m) in the Halahatang area, Tarim Basin (Modified from [30]).

On the basis of seismic responses analysis, the integrated application of coherent enhancement technique, Automatic Fault Extraction (AFE, Figure 3b) and other seismic attributes are useful for carbonate fault “damage zone” identification under the deep subsurface [31]. The result of this analysis showed that carbonate fault damage zones are widely distributed as fan-shape features along the fault zone, generally with a width of 200–2500 m (Figure 3b) [30,31]. These fault damage zones have good agreement with the high well production within 1200 m of the fault cores [30]. In more than 200 wells, that penetrated the Ordovician carbonates, almost all wells attained a high productivity fall into fault damage zones, although some of the wells still yield a low productivity in the damage zones [30,31].

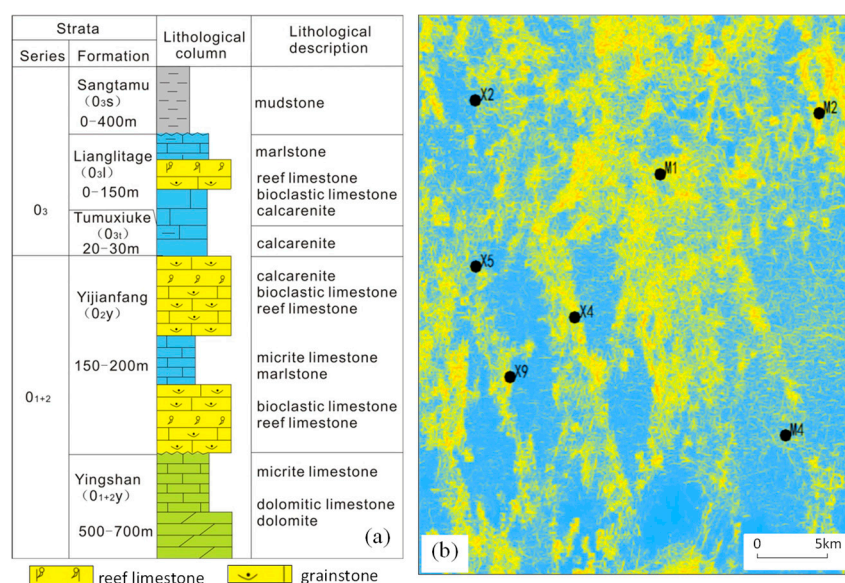


**Figure 3.** (a) Stratigraphic column of the Ordovician carbonate in the Halahatang area, China, and (b) Automatic Fault Extraction (AFE) description of the damage zones (yellow areas) affecting the Ordovician carbonate (after [31]) in this area (the black dots show well locations).

In the Halahatang study area, the top of the Ordovician was buried at a depth of 6500–7500 m and dips gently towards the south of the basin (Figure 1b) [28]. The primary reservoirs of the Yjianfang Formation are mainly reef-shoal facies in a broad ramp platform [28,32], with a thickness of up to 200 m (Figure 3a). The bulk of the carbonate reservoirs are rich in grainstones, formed from the large shoal facies interbedded with small reefs [28]. There are large areas of tight carbonates in the broad slope that has a very low matrix porosity (<5%), and low permeability (<1 mD), with considerable heterogeneity [28]. The major production in this area is from dissolution vugs (diameter between 2–100 mm) and caves (diameter >100 mm) found in the tight matrix carbonate reservoirs [28,33]. The "sweet spots" of fracture-cave reservoirs (assemblages of caves, vugs and fractures) showing "bead-shape" strong reflection in the seismic profile [28]) are main targets for the production in the carbonate reservoirs [29,33,34]. The fracture-cave reservoirs are quite different from the high matrix reservoirs and meteoric karst reservoirs [35,36], but are strongly heterogeneous reservoirs that are close to hypogene or hydrothermal karstification along fault zones [37–39].

### 3. Data and Methods

Cores were available for study from more than 20 wells penetrating the Halahatang area Ordovician carbonates along the fault damage zones. These enable core and thin section data to be used in describing the microstructures and structure related diagenesis in the carbonate fault zones. We analyzed the sequence of the fractures by examining cross-cutting and termination relationships, filling and cement generations, and orientation in cores and thin section samples. Pink-dye resin impregnated thin sections were used to identify porosity. FMI (micro-resistivity image logging) allowed for fracture orientation analysis [30]. These measurements were used to discuss the fracture paragenetic sequence. Together with the timing constrains by fault activities, we present a relatively paragenetic sequences of structural diagenesis in the carbonate fault damage zones. In contrast to the diagenesis in the country rocks, we discuss the faulting impacts on the diagenesis along the carbonate fault damage zones in the Tarim Basin.

## 4. Structure Related Diagenesis

### 4.1. Compaction and Pressure Solution

The Ordovician country rocks, in the deep subsurface (>6000 m), exhibit evidence of strong compaction with line and edge contacts among the mineral grains in the carbonates (Figure 4a) [28,40]. In the fault damage zones, some thin sections show floating and point contacts of the grainstones (Figure 4b), and point and line contacts in other grainstones (Figure 4c). The variable compaction in the carbonate fault damage zones is inconsistent with the relatively strong and uniform compaction in the host rocks. In this context, the fault activity possibly had an impact on the carbonate diagenesis in the fault damage zones.

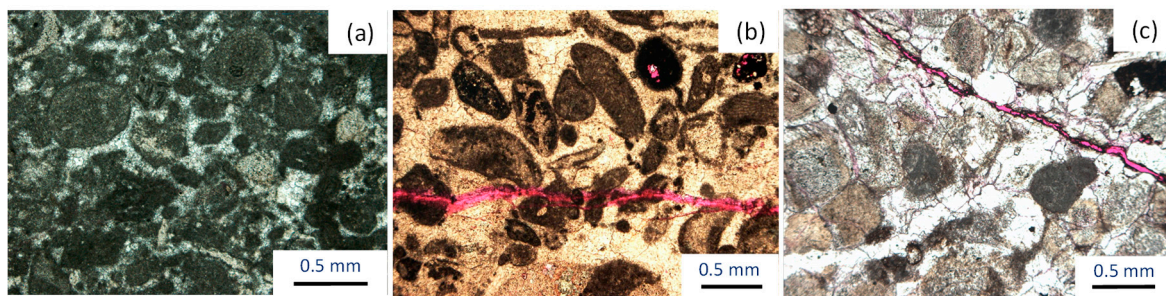


**Figure 4.** Photomicrographs showing compaction observed in the thin sections (pink-dye resin impregnated to better illustrate sample porosity). (a) Grainstone showing line contacts in country rocks, H6-1, 6667.93 m; (b) floating grains in grainstone showing weak compaction in a fault damage zone, H7-3, 6644.47 m; (c) strong compaction and recrystallization in a fault damage zone, H803, 6578 m.

Pressure solution is evident by the common occurrence of stylolites [41,42] in the Halahatang area Ordovician carbonate rocks (Figure 5). Bedding-parallel stylolites occur throughout the studied succession of carbonates. The stylolites exhibit different morphologies. Many bedding-parallel stylolites (S1-1) were observed in core with low amplitude, wave-like profiles. Some stylolites (S1-2) have higher amplitudes forms, rectangular layer type and seismogram pinning type, and low intersection angles with the strata and bedding-parallel stylolites (S1-1) (Figure 5a,b). These stylolites (S1-2) merge and overprint those of the bedding-parallel stylolites (S1-1), suggesting a postdate pressure solution [43]. Stylolites were encountered mainly in wackstone-packstone rather than in sparry cement grainstones, which suggests a lithological control on pressure solution. Some stylolites (S2) are perpendicular or oblique to bedding (Figure 5b,c). These stylolites are generally classified as tectonic stylolites with surfaces perpendicular to the largest compressive principal stress axis [43]. The tectonic stylolites are generally sub-perpendicular to, terminate or intersect with the bedding-parallel stylolites. Most tectonic stylolites have low-amplitudes and sharp peaks. They are typically enlarged and partial filled with calcite cements and arenopelitic fillings. In the country rocks, there is generally one set of bedding-parallel stylolites with serrate or wave-like profiles within cores (Figure 5d). These features suggest a complicated diagenesis for the observed stylolites in the fault damage zones in contrast to the tight stylolites in the host carbonate rocks.

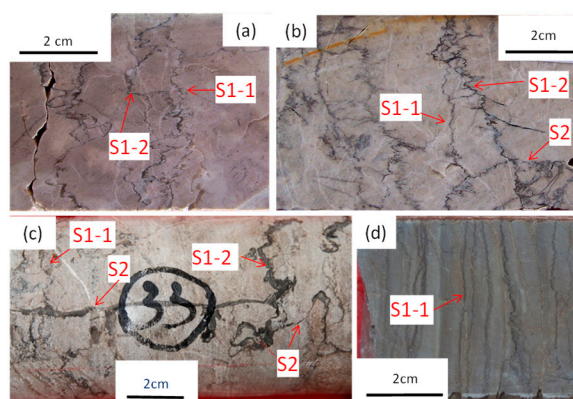


**Figure 5.** Photographs showing stylolites in cores. (a) Bedding-parallel, low-amplitude stylolite (S1-1) and high-amplitude stylolite (S1-2), H601-1, 6633.28 m; (b) oblique stylolite (S1-2) merged into bedding-parallel stylolite (S1-1), tectonic stylolite (S2) terminated in the oblique stylolite (S1-2), H902, 6641.61 m; (c) tectonic stylolite (S2) cross-cutting S1-1 stylolites and terminated in S1-2 stylolites; dissolution and enlargement along S1-2 and S2 stylolites in a fault damage zone, R4, 6625 m; (d) bedding-parallel stylolites (S1-1) in mudstone in country rocks, H6, 7044.21 m.

#### 4.2. Cementation

The primary porosity of the Halahantang area Ordovician carbonate rocks is almost completely occluded (Figures 4 and 6a) [28,40]. The secondary porosity in fractures and vugs is also filled mainly by calcite cements and some bitumen (Figure 6). Thin section analysis reveals that the early sparry cements generally hindered further compaction (Figures 4 and 6a), suggesting that compaction and cementation were synchronous with early shallow burial depths. The country rocks are characterized by fine-grained, thin, equidimensional cements (C1-1) surrounding the grains, and coarser, equant, granular cements (C1-2) that infilled in the intergranular porosity (Figure 6a). The fine cements coating the grains are assumed to have occurred in a marine diagenetic environment [28,40]. As such, there were possibly multiple cementation generations affecting the intergranular porosity of the Ordovician carbonate in the Tarim Basin [40], but herein we only discuss those that are related to fault activity.

In the fault damage zones, there were generally observed 2-4 generations of calcite cement [28] (Figure 6). The intergranular cements (C1-2) are cut by later fractures (Figure 6b) [28,30], suggesting local fault related cements occurred after the eogenetic cementation (C1). Two stages of cement were observed within the fractures (Figure 6c,e) from the fault zones, as well as in the vugs [28]. Veins within fractures are generally filled with coarse blocky cements (C2) towards their center, and finer, calcite cements (C3) along fracture walls (Figure 6c), suggesting the fracture enlarged and precipitating the coarse calcite cements in the center, post crystallization of the narrow, finer calcite along the fracture wall. In the sample thin sections (Figure 6d), a late vein (C3) terminated an earlier generation of veins (C2) possibly indicating a late stage of cementation. In addition, bitumen impregnated cements (C3) divided by early white cements (C2) in the fracture center also favor at least two stages of vein cementation (Figure 6e). These early vein cements (D2) are generally wider than the late cements (D3), consistent with a stronger fault activity in the early stage [29,30]. The early vein cements are generally fully infilled and are cross-cut or overprinted by the latest fractures (Figure 6f), although the latest fractures have little by way of cement (D4). These observations attest to at least three generations of pore/fracture cementation (C2-C4), following on from the main stage of compaction and cementation (C1) during eogenetic environment.

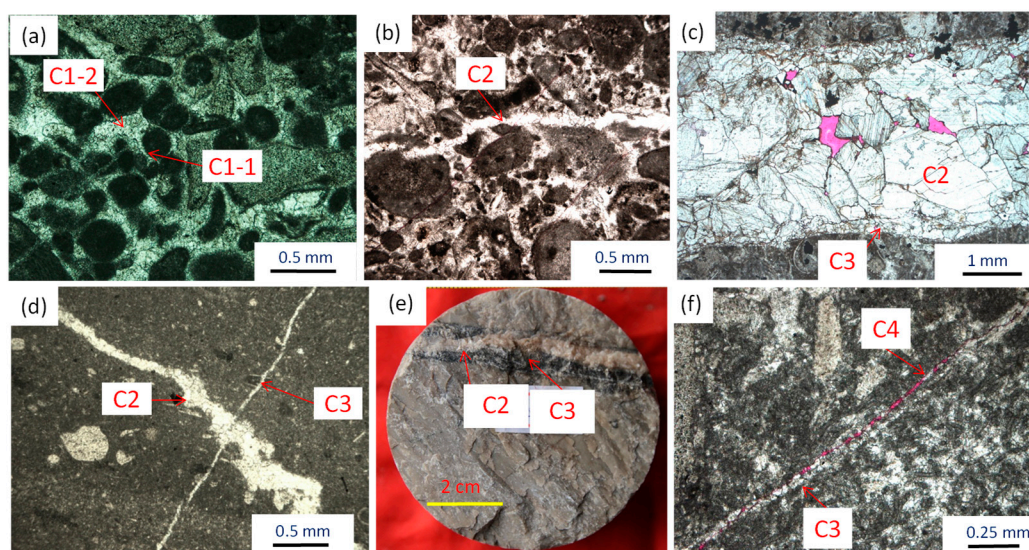


**Figure 6.** Photographs and photomicrographs illustrating cementation and dissolution textures observed in core (e) and thin section samples (a–d,f) of the Ordovician carbonates in the Halahatang area (pink-dye resin impregnated to better show fracture porosity). (a) Fine cements (C1-1) with isopachous coating the grains, coarse granular cements (C1-2) within the intergranular porosity in the country rocks, X101, 6822.08 m; (b) the late fracture filled cements (C2) cut across and overprinted the early intergranular cements (C1), H7-1, 6579.58 m; (c) two stages of cementation filling in a micro-fault, with earlier wide cements (C2) in the center separated the narrow fine cements on the wall (C3), H803, 6598.85 m; (d) a narrower cement vein (C3) terminated on a wider vein (C2), H11-1, 6683 m; (e) a white cement (C2) occurring in the fracture center divides the bitumen impregnated cements (C3) to highlight two stages of cementation, H801, 6733.6 m; (f) late partially filled cements (C4) in the fracture cuts across and merged with the earlier fully cemented (C3) fracture, H7-1, 6581.22 m.

#### 4.3. Fracturing

Multiple fractures developed upon a wide fault damage zone with a width of more than 2 km, in the carbonate rocks in Halahatang area [30,31]. The fractures mainly have steep dips ( $> 60^{\circ}$ ) as observed in core and FMI images [29,30] (Figure 7a–c). Analysis of thin sections and cores (Figure 7d–f) shows that there are generally two sets of fractures developed in the Ordovician carbonate rocks. FMI image analysis also revealed two sets of fractures in this area [30], striking NE and NW, which is subparallel to the strike-slip faults throughout the study area (Figure 2b). Some of the conjugate fractures and en echelon fractures are similar to those of the fault system [30], suggesting the self-similarity between the fault system and its microstructures. In general, only one set of fractures developed preferentially in a well. Most fractures have narrow aperture (Figure 7a); some show wider aperture, particularly in multiple reactivated fractures (F1 in Figure 7b,c). The fracture apertures generally range from 0.1 mm to 5 mm in core, and 0.005 to 0.1 mm in sample thin sections. A few veins with aperture values of more than 1 cm were observed in core. The fractures are characterized by multiple enlargements and almost all are completely infilled by calcite cement(s) (F1 in Figure 7a–c), and arenopelitic fillings and bitumen (F2 in Figure 7b,c). A few fractures are partially calcite-filled and host bitumen.

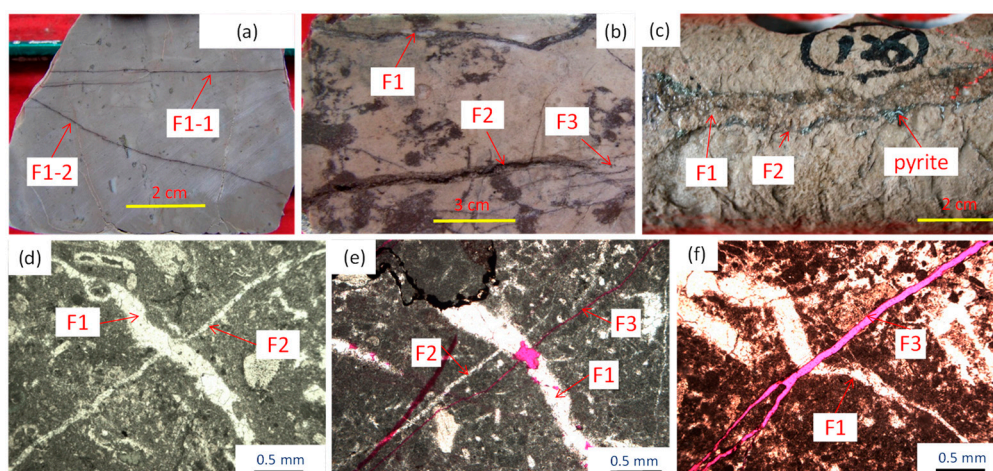


**Figure 7.** Photographs and photomicrographs showing fractures in the cores (a–c) and thin sections (d–f) of the Ordovician carbonates in the Halahatang area. (a) One vertical fracture (F1-1) and one high angle fracture (F1-2) showing a narrow aperture and cements filling, H902, 6632.12 m; (b) high angle fractures infilled by calcite cements (F1), reactivated open fracture filled with bitumen (F2) and late subparallel fractures at the tip (F3), H601-1, 6634.40 m; (c) an early cemented fracture (F1) reactivated (F2) along the fracture wall and splits the argillaceous and pyrite cements, X101, 6767.52 m; (d) an early wider, enlarged fracture (F1) terminated a late narrower fracture (F2), H11-1, 6682.5 m; (e) cross-cutting relationship showing early wide fracture (F1) terminated the second generation fracture (F2), and cut across by the latest open fracture (F3), J7, 7108.6 m; (f) late open fracture (F3) cuts across the former earlier, fully infilled fracture (F1), X7, 6918.12 m.

Fracture cross-cutting relationships and the cementation sequence in the core and sample thin sections suggest there were multiple stages of fracturing (Figures 6d–f and 7). The fracture enlargement and fillings show at least two stages of fracturing in the fault damage zones (Figures 6c and 7b,c). The first fracturing episode (F1) was almost all completely infilled by coarse calcite cement. A second stage of fracturing (F2) led to the enlargement of early fractures (F1) and initial cement cements (C2) (Figure 6c) with those of a narrower aperture and finer cement. Some of the second fractures (F2) have been distorted (Figure 7d and terminated (Figure 7e) by the earlier fractures (F1), and/or overprinted (Figure 6c,e and Figure 7b) in the earlier fractures (F1). The first stage fractures (F1) generally have wider aperture than the second stage fractures (F2) (Figure 7b–e), consistent with the wider early cements (C2) (Figure 6c,d). These fractures are almost completely filled with calcite cement. In contrast, most of the late stage fractures (F3) that cross cut F1 and F2 fractures are open with fewer fillings (Figure 7e,f). The late fractures (F3) have somewhat enlarged earlier cemented fractures (Figure 7b).

#### 4.4. Dissolution

The primary porosity of the Ordovician carbonate rocks from the Halahatang area has been almost totally occluded during burial diagenesis [28,40]. Reservoir porosity is primarily the result of dissolution [28,30,33,34]. Multiple dissolution events have affected the carbonate rocks in the fault damage zones whereby the dissolution porosity occurs along the fractures (Figure 8a), along rectangular stylolites (Figure 8b), and within the cataclases (Figure 8c). Although many bedding-parallel stylolites (S1-1) were completely infilled to be effective barriers to fluid flow, some stylolites have been reactivated to create some porosity and permeability in these rocks (Figures 5b and 8b). Note that much more dissolution vugs and pores are associated with tectonic stylolites rather than the sub-parallel stylolites (Figure 5c), suggesting a stronger reactivation and dissolution of the tectonic stylolites.

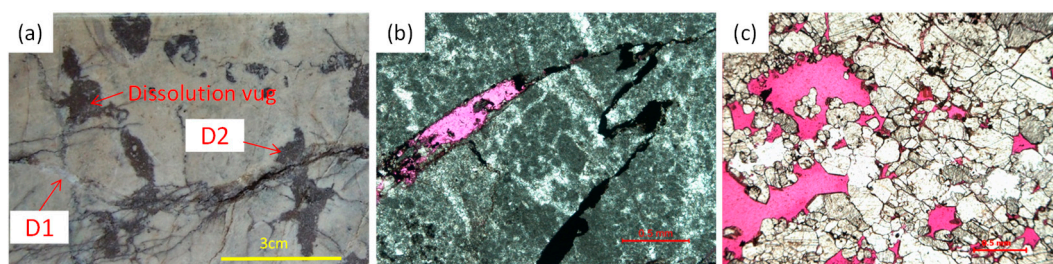


**Figure 8.** Photographs showing dissolution in the carbonate fault damage zones in the Halahatang area (the pink-dye resin showing the porosity). (a) Multiple dissolution in cores, the first dissolution (D1) porosity is occluded by calcite cements, the second dissolution (D2) porosity and vugs are filled with cements and bitumen, the late fracture (under arrow of D2) reactivation and opening possibly suggest third stage dissolution; H601-1, core, 6638 m; (b) dissolution porosity along a stylolite, H601-18, thin section, 6755.04 m; (c) dissolution porosity among the cataclasites, H803, thin section, 6573.78 m.

The vein cementation is closely related to dissolution (Figure 6b,d), which likely provided saturated waters with calcite for cementation [44]. It is noted that the reactivated fractures are closely related to dissolution features, formed during fracture enlargement (Figures 7b and 8a). Thus, the wider aperture was generally furnished by the dissolution episode. Pervasive cementation occurred during F1 and F2 fracturing, as indicated by dissolution (Figures 6 and 7). Unfortunately, residual porosity is still poor as a result of the intense cementation during F1 and F2 fracturing, particularly the case in the wider fractures near fault cores. There is generally weaker dissolution associated with the F3 fractures and accordingly little cementation along these late fractures (Figure 7e,f).

## 5. Discussion

### 5.1. Paragenetic Sequence of the Structure Related Diagenesis

The relative paragenetic sequences of diagenesis are possibly inferred from fracture cross-cutting and abutting relationships and orientations, and the observed cementation relationships [9,22,40,45,46]. With reference to the identified relationships and orientation(s) of fracture cross-cutting and abutting, styles of cements and evident dissolution generations (Figures 5–8), three stages of fracture development and cement precipitation in the fracture zones are suggested, and which may be consistent with three cycles of fault activity [29,30]. Over the long history of multi-stages tectonic and fault activities affecting the Ordovician Halahatang area carbonate sequence [29,30], four stages of diagenesis were documented in this study, in those carbonate rocks of the fault damage zones (see Figure 9).

Diagenetic settings can be subdivided into marine, eogenetic and mesogenetic environments [7,40,47]. The first-generation cements (C1-1) observed in the carbonate rocks are marked by fibrous cements (Figure 6a), generally in the form of isopachous grain coatings, and are consistent with the marine environment in the Tarim Basin [28,40]. The subsequent granular and stalactitic cements (C1-2) (Figures 4 and 6a) are characterized by fabric-selective dissolution, suggesting an early eogenetic environment [40]. Although there are multiple stages of cementation in the intergranular porosity of the Ordovician carbonate rocks, most of the cementation occurred in a marine to eogenetic environment [28,40]. The intergranular cements are generally cross-cut by the fractures (Figure 4b,c), as well as by the stylolites (Figure 8b). Thus, most of the cements likely formed during the early stages of diagenesis, prior to faulting activity. In the shallow burial, eogenetic environment, compaction was initiated, and following two subsequent phases of bedding-parallel stylolite formation (S1-1 and S1-2), led to the sequence of carbonate rocks becoming progressively more compacted with depth.

During the first episode of fracturing, tectonic stylolites commonly cut across horizontal stylolites (Figure 5b,c) suggesting that fracture initiation began after S1-1 and S1-2 [41,42]. In the core and sample thin sections, the tectonic stylolites are cross-cut by later fractures. Some tectonic stylolites are reactivated by and absorbed into the later fractures (Figure 6b). In general, the early fractures have

wide aperture, and pervasively occluded the primary pores by cements (Figures 6c–e and 7d,e). The dissolution along the early fractures is relatively weak compared to the intense early cementation.

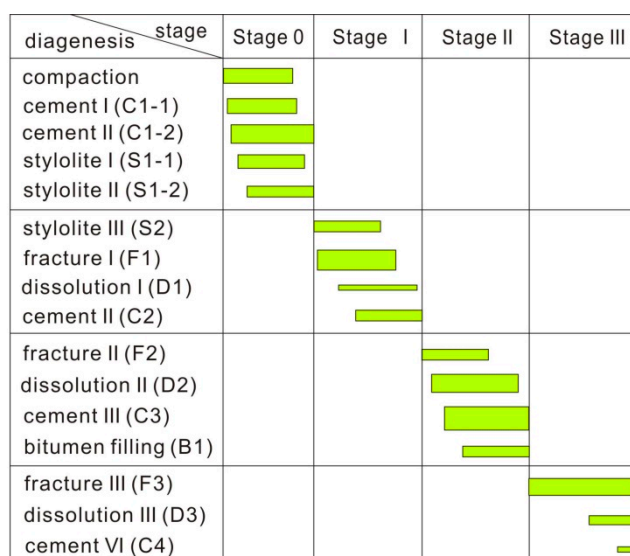


**Figure 9.** Paragenetic sequences of diagenesis affecting the Ordovician carbonate rocks in the fault damage zones of the Halahatang area. The length and height of each green bar is representative of the relative duration and magnitude of event, respectively. The diagenetic sequences from stage 0 are those that likely to have occurred early, during burial and compaction (i.e., an eodiagenetic setting) prior to the onset of fault activity. Some stylolites (S1-2) with small dip angles to bedding possible indicate the initiation of fault activity. Stages I–III possibly correspond to the fault activities occurring during the Late Ordovician, Permian and Cenozoic eras (Figure 2a) [29,30].

In the second stage of fracturing (Figure 7), the later fractures (F2) generally were terminated or distorted at the intersection with early fractures (F1). The fracture enlargement and dissolution are ubiquitous in the carbonate rocks of the study area (Figure 7b,c), and subsequent cements infilled a narrower aperture than for the early cements. These observations suggest intense fluid activity which had a dominant influence on the precipitation of calcite during the carbonate diagenesis (cementation) in the fault damage zones. This is consistent with the documented extensive, hydrothermal activity during the Permian throughout the Tarim Basin [48,49]. Almost all of the porosity in the first and second fractures has been occluded by strong precipitation of calcite cements during deep burial environment (Figures 6 and 7).

We observed open/uncemented microfractures (F3) overprinting across all the earlier cemented fractures (Figure 7), suggesting a latest stage fracture activity that is not related to strong diagenesis. The cross-cutting relationship for this episode possibly suggests that the tectonic stress field had changed, from the approximately NNE directional compression in the late Ordovician [29] to the NNW directional extension in the Eocene [25,27], for the new orientation fracture initiation. There is also observed fracture enlargement, but weak dissolution in this latest stage of fracture (Figures 7b and 8a).

Following multiple phases of structural diagenesis (Figure 9), late fractures can overprint those early fracture textures, modifying and/or inheriting from their pre-existing fracture traces and ultimately superimposing upon these diagenetic features a new phase of fracture activity.

## 5.2. Fault Controls on the Structural Diagenesis

Together with the macro- and micro-structures observed in the Halahatang area Ordovician carbonates [28,40,48–50], there are multiple features that evidence the complicated structural control upon diagenesis rather than that which typifies the relatively uniform diagenesis of the carbonate country rocks unaffected by faulting (Table 1). The fracture elements present and production data [30]

have shown the structure-related diagenesis is constrained to within the fault damage zones, or their immediate vicinity, with those rocks productivity controlled by the fault activities.

**Table 1.** A comparison of diagenesis between fault damage zones and country rocks.

Diagenesis	Country Rocks	Damage Zone
Compaction	relatively strong, line/serrate contacts	multiple point/line/serrate contacts
Pressure solution	1–2 stages, serrate and wave-like profiles, bedding-parallel stylolites; tight	2–3 stages, bedding-parallel and inclined stylolites and 1–2 stages tectonic stylolites, localized dissolution porosity and bitumen infill
Fracturing	undeveloped, one set of regional sub-vertical fracture, calcite infill/cementation, little dissolution of porosity	2–4 stages, multiple kinds and orientations of fractures, partial filling/cement, multiple-stages of dissolution enhancing porosity
Cementation	1–2 stages of marine cements, 1–2 stages eogenetic-mesogenetic cements, strong cementation and little dissolution	2–5 stages eogenetic-mesogenetic cements, relatively weak cementation and multiple-stages of dissolution
Dissolution	a few burial dissolution, dissolution porosity occluded by cements	2–4 stages dissolution, development of partially filled porosity, vugs and caves

Previous studies have shown that the Ordovician limestones in the Tarim Basin have undergone more than 10 generations of diagenesis in the submarine, eogenetic and mesogenetic environments [28,40,48–50]. In these studies, multiple episodes of fracture activity and/or hydrothermal activity evidenced in the Ordovician carbonates are correlated to fault activities in the Tarim Basin [28,49,51]. Meteoric dissolution and cementation are sparse in the country rocks, although some are possible related to penecontemporaneous diagenesis [48,50] and most can be related to an unconformity [51]. In the Halahatang area, the arenopelitic fillings observed in the fault damage zone samples collected as part of this study suggest a fault related meteoric diagenesis. By comparison analysis, more than three additional stages of cementation and dissolution can be identified atop of those present from the burial diagenesis, with these likely being related to structural activity, as compared to most country rocks that generally had only 1–2 stages of cementation (Figures 4a and 6a), but little dissolution [28,40,48–51]. In this context, the complicated diagenetic processes are almost all related to fault activity, other than those resulting from the depositional and burial diagenesis in the Ordovician carbonate rocks. In the deep and long burial history, the host rocks generally had strong compaction, 1–2 stages of bedding-parallel stylolites, 1–2 stages of submarine and 1–2 stages of burial cementation, and little fracture and dissolution porosity in Halahatang area (Table 1, Figures 4–8). This is consistent with other areas in the Tarim Basin [28,40,48–51].

On the other hand, there are complicated compaction and pressure solution, multiple fracturing and cementation and dissolution along the fault damage zones of the Halahatang area (Table 1). The limestones show a relatively uniform compaction with line contact in the grainstones and packstones in the country rocks [28,40], but both strong and weak compaction in the fault damage zones (Figure 4b,c). The relatively strong compaction is not only related to lithology, but also possibly affected by the fault tilting and transpressional stress regime operating during the fault activity [29], whereas some rocks in the damage zones show relatively weak compaction with point/line contact between the grains (Figure 4b). The weak compaction with grainstones floating in the cements is possibly related to slow subsidence and rapid cementation during the early fault activity related uplift. In addition, the inhomogeneous early cementation and overpressure fluid(s) may inhibit the compaction process [7,52]. Except for bedding-parallel stylolites, inclined, vertical and cross-cutting types of stylolites were observed in the fault damage zones (Figure 5a–c), but were absent in the country rocks (Figure 5d). In addition, the bedding-parallel stylolites in the damage zones have relatively larger amplitudes than those of the country rocks. These features suggest a stronger degree of pressure solution in fault damage zones. Tectonic (transverse) stylolites were mainly observed perpendicular to bedding, whereas, some inclined and irregular stylolites suggest complicated compressional stress in the fault damage zones. The stylolites are tight in the country rocks, but some stylolites were reactivated and

have residual porosity (Figure 5a,b). In addition, there are some evidence of dissolution porosity, and cements and bitumen infill along with the stylolites (Figure 8b), suggesting a preferred pathway of the stylolites for fluid flow, corrosion and mineralization during this diagenetic stage. These reactivated stylolites in the damage zones are favorable for fluid interaction by locally increasing the porosity and permeability above that of the tight stylolites in country rocks. The reactivation of the stylolites is closely related to multiple faulting activities, while the origin and mechanism of these activities requires further study.

Fracture processes have been systematically investigated along the fault zones [9,11,15,24]. In this area, there is generally sparse fractures (less than one in two meter cores) occurred from the boreholes in the country rocks. However, in the damage zones, there are multiple kinds (Figures 5–7) and dense fractures with fracture frequency more than 50 in one meter cores [30]. The fractures mainly distributed in the fracture zone within 2 km of the fault zone [30,31]. Following multiple fault activities, the fractures are characterized by 2–3 periods reactivation, as well as multiple dissolution and cementation (Figures 6–8). Three stages fracturing (Figure 7) suggest three cycles of fracture opening and sealing. It is noteworthy that the latest fractures (F3) are almost opening, but the early fractures (F1 and F2) are mostly sealed. Nonetheless, the fractures varied in patterns, frequency, parasequence and petrophysical properties [30] with spatio-temporal change in the fault zones. These suggest strong anisotropy and heterogeneity of the fracturing and associated diagenesis in the fault zones.

In the fault damage zones, there are complicated carbonate cementation and dissolution features observed (Figures 6–8). Except for the early depositional diagenesis, the later three stages of cementation and dissolution may be related to the fault activity in the fault damage zones (Figure 9). Previous studies have documented 2–3 generations of strong cementation among the grainstones, but little dissolution in the country rocks [28,40]. In the fault damage zones, additional 3 stages of calcite cementation have pervaded the fractures and cataclastic rocks (Figures 6 and 7). The strong cementation of early two stages cements (C2 and C3) may correspond to a rapid subsidence following early fault activities [28–30]. In addition, the hydrothermal activity possible increased the calcite precipitation [48,49,51], considering the damage zone is favorable for fluid flow and mineral precipitation [5,14,17]. On the other hand, the latest fracture family (F3) is possible related to Eocene fault activity, prior to the onset of large scale cementation. In the Halahatang area, most primary porosity has been occluded by the strong cementation during the long burial history of these rocks (Figure 4) [28,40]. The microstructures present show more than 90% porosity is of dissolution porosity (Figures 5–8). This is consistent with the fact that the Ordovician carbonate reservoirs are mainly characterized by dissolution vugs and caves [28,33,34], and almost all occur along the fault damage zones [30,31]. Regardless of the intense cementation, there is much stronger dissolution in the fault damage zones (Figure 8) than the country rocks (Figures 4a and 6a). This suggests the dissolution porosity mainly occurred within the fault damage zones, although it is still ambiguous for the process of the large caves [34]. There is generally a complicated interplay between cementation and dissolution as a consequence of mechanical deformation in the Ordovician carbonates [7,13,14,53]. In this study, much more dissolution developed along the fault damage zones, suggesting fluid pathways formed in those areas facilitating the later dissolution in the fault zones.

## 6. Conclusions

Although the carbonate diagenesis within fault damage zones is difficult to predict in the subsurface, we propose the following model, based upon an integrated analysis of the carbonate fault damage zones in the Tarim Basin (Halahatang area).

1. Multiple phases of carbonate diagenesis in the fault damage zones may be identified from the subsurface based upon stylolite type and fracture cross-cutting relationships, fracture orientations and cementation generations in the sedimentary basin strata.
2. The country rocks have undergone strong compaction, pressure solution and cementation, during deep burial, but few fracture and dissolution porosity features are evident in the Ordovician

carbonates in this study area. However, there are complicated compaction, 1-2 stages of tectonic stylolites, 2-4 stages fractures and associated cementation and dissolution in these same carbonates found along the fault damage zones.

3. In contrast to the country rocks, this study suggests an additional three cycles of structural diagenesis occurred within the carbonate fault damage zones. The two early stages of fracture activities are followed by strong cementation, while much more open fracture is characteristic of the latest stage of brittle deformation.
4. The carbonate structure related diagenesis is constrained to the fault zones, and its spatio-temporal distribution and variation are mainly controlled by the three different stages of fault activities affecting these rocks.

**Author Contributions:** G.W., Y.Z. and E.X. conceived the study; E.X., X.L. and C.S. collected samples and analyzed the data; G.W., Y.Z. and H.Q. discussed and interpreted the results; G.W. and H.Q. wrote the paper with contribution from all authors.

**Funding:** National Natural Science Foundation of China (Grant No. 41472103) and National Science and Technology Major Project (2011ZX05004001).

**Acknowledgments:** We thank the Tarim Oil Company for data support and project research. We are grateful to Professor Ian Coulson and DCP Peacock for their constructive comments and careful revisions of the manuscript that substantially improved the manuscript. We also thank Lixin Chen, Xiaoguo Wan, Guohui Li, Kuanzhi Zhao and Lianhua Gao for their help for data analysis and interpretation.

**Conflicts of Interest:** The authors declare no conflict of interest.

## References

1. Faulkner, D.R.; Jackson, C.A.L.; Lunn, R.J.; Schlische, R.W.; Shipton, Z.K.; Wibberley, C.A.J.; Withjack, M.O. A review of recent developments concerning the structure, mechanics and fluid flow properties of fault zones. *J. Struct. Geol.* **2010**, *32*, 1557–1575. [[CrossRef](#)]
2. Bense, V.F.; Gleeson, T.; Loveless, S.E.; Bour, O.; Scibek, J. Fault zone hydrogeology. *Earth Sci. Rev.* **2013**, *127*, 171–192. [[CrossRef](#)]
3. Trippetta, F.; Carpenter, B.M.; Mollo, S.; Scuderi, M.M.; Scarlato, P.; Collettini, C. Physical and transport property variations within carbonate-bearing fault zones: Insights from the Monte Maggio Fault (Central Italy). *Geochem. Geophys. Geosyst.* **2017**, *18*, 4027–4042. [[CrossRef](#)]
4. Caine, S.J.; Evans, J.P.; Forster, C.B. Fault zone architecture and permeability structure. *Geology* **1996**, *24*, 1025–1028. [[CrossRef](#)]
5. Kim, Y.S.; Peacock, D.C.P.; Sanderson, D.J. Fault damage zones. *J. Struct. Geol.* **2004**, *26*, 503–517. [[CrossRef](#)]
6. Peacock, D.C.P.; Dimmen, V.; Rotevatn, A.; Sanderson, D.J. A broader classification of damage zones. *J. Struct. Geol.* **2017**, *102*, 179–192. [[CrossRef](#)]
7. Moore, C.H. Carbonate Diagenesis and Porosity. In *Developments in Sedimentology*; Elsevier Science Publishers: Amsterdam, The Netherlands, 1989.
8. Wilson, J.E.; Goodwin, L.B.; Lewis, C. Diagenesis of deformation band faults: Record and mechanical consequences of vadose zone flow and transport in the Bandelier Tuff, Los Alamos, New Mexico. *J. Geophys. Res.* **2006**, *111*, B09201. [[CrossRef](#)]
9. Laubach, S.E.; Eichhubl, P.; Hilgers, C.; Lander, R.H. Structural diagenesis. *J. Struct. Geol.* **2010**, *32*, 1866–1872. [[CrossRef](#)]
10. Laubach, S.E.; Ward, M.W. Diagenesis in porosity evolution of opening-mode fractures, Middle Triassic to Lower Jurassic La Boca Formation, NE Mexico. *Tectonophysics* **2006**, *419*, 75–97. [[CrossRef](#)]
11. Olson, J.E.; Laubach, S.E.; Lander, R.H. Natural fracture characterization in tight gas sandstones: Integrating mechanics and diagenesis. *AAPG Bull.* **2009**, *93*, 1535–1549. [[CrossRef](#)]
12. Rath, A.; Exner, U.; Tschegg, C.; Grasemann, B. Diagenetic control of deformation mechanisms in deformation bands in a carbonate grainstone. *AAPG Bull.* **2011**, *95*, 1369–1381. [[CrossRef](#)]
13. Hooker, J.N.; Gomez, L.A.; Laubach, S.E.; Gale, J.F.W.; Marrett, R. Effects of diagenesis (cement precipitation) during fracture opening on fracture aperture-size scaling in carbonate rocks. *Geol. Soc. Lond. Spec. Publ.* **2012**, *370*, 187–206. [[CrossRef](#)]

14. Hodson, K.R.; Crider, J.G.; Huntington, K.W. Temperature and composition of carbonate cements record early structural control on cementation in a nascent deformation band fault zone: Moab Fault, Utah, USA. *Tectonophysics* **2016**, *690*, 240–252. [[CrossRef](#)]
15. Williams, R.T.; Goodwin, L.B.; Mozley, P.S. Diagenetic controls on the evolution of fault-zone architecture and permeability structure: Implications for episodicity of fault-zone fluid transport in extensional basins. *GSA Bull.* **2017**, *129*, 464–478. [[CrossRef](#)]
16. Knipe, R.J. The influence of fault zone processes and diagenesis on fluid flow. In *Diagenesis and Basin Development (AAPG Studies in Geology)*; Horbury, A.D., Robinson, A.G., Eds.; American Association of Petroleum Geologists: Tulsa, OK, USA, 1993; pp. 135–154.
17. Eichhubl, P.; Davatzes, N.C.; Becker, S.P. Structural and diagenetic control of fluid migration and cementation along the Moab fault, Utah. *AAPG Bull.* **2009**, *93*, 653–681. [[CrossRef](#)]
18. Yielding, G.; Bretan, P.; Freeman, B. Fault seal calibration: A brief review. *Geol. Soc. Lond. Spec. Publ.* **2010**, *347*, 243–255. [[CrossRef](#)]
19. Vandeginste, V.; Swennen, R.; Allaey, M.; Ellam, R.M.; Osadetz, K.; Roure, F. Challenges of structural diagenesis in foreland fold-and-thrust belts: A case study on paleofluid flow in the Canadian Rocky Mountains West of Calgary. *Mar. Pet. Geol.* **2012**, *35*, 235–251. [[CrossRef](#)]
20. Pei, Y.; Paton, D.A.; Knipe, R.J.; Wu, K. A review of fault sealing behaviour and its evaluation in siliciclastic rocks. *Earth Sci. Rev.* **2015**, *150*, 121–138. [[CrossRef](#)]
21. De Graaf, S.; Reijmer, J.J.G.; Bertotti, G.V.; Bezerra, F.H.R.; Cazarin, C.L.; Bisdorn, K.; Vonhof, H.B. Fracturing and calcite cementation controlling fluid flow in the shallow-water carbonates of the Jandaíra Formation, Brazil. *Mar. Pet. Geol.* **2017**, *80*, 382–393. [[CrossRef](#)]
22. Petrie, E.S.; Petrie, R.A.; Evans, J.P. Identification of reactivation and increased permeability associated with a fault damage zone using a multidisciplinary approach. *J. Struct. Geol.* **2014**, *59*, 37–49. [[CrossRef](#)]
23. Eichhubl, P.; Boles, J.R. Rates of fluid flow in fault systems - evidence for episodic rapid fluid flow in the Miocene Monterey Formation, coastal California. *Am. J. Sci.* **2000**, *300*, 571–600. [[CrossRef](#)]
24. Gratier, J.-P. Fault permeability and strength evolution related to fracturing and healing episodic processes (years to millennia): The role of pressure solution. *Oil Gas Sci. Technol.* **2011**, *66*, 491–506. [[CrossRef](#)]
25. Jia, C.Z. *Tectonic Characteristics and Petroleum, Tarim Basin, China*; Geological Publishing House: Beijing, China, 1997; pp. 29–261. (In Chinese)
26. Li, Q.M.; Wu, G.H.; Pang, X.Q.; Pan, W.Q.; Luo, C.S.; Wang, C.L.; Li, X.S.; Zhou, B. Hydrocarbon accumulation conditions of Ordovician carbonate in Tarim Basin. *Acta Geol. Sin.* **2010**, *84*, 1180–1194.
27. Tang, L.J.; Huang, T.Z.; Qiu, H.J.; Wan, G.M.; Li, M.; Yang, Y.; Xie, D.Q.; Chen, G. Fault systems and their mechanisms of the formation and distribution of the Tarim Basin, NW China. *J. Earth Sci.* **2014**, *25*, 169–182. [[CrossRef](#)]
28. Du, J.H. *Oil and Gas Exploration of Cambrian-Ordovician Carbonate in Tarim Basin*; Petroleum Industry Press: Beijing, China, 2010. (In Chinese)
29. Wu, G.H.; Yuan, Y.J.; Huang, S.Y.; Vandyk, T.M.; Xiao, Y.; Cai, Q.; Luo, B.X. The dihedral angle and intersection processes of a conjugate strike-slip fault system in the Tarim Basin, NW China. *Acta Geol. Sin. Engl. Ed.* **2018**, *92*, 74–88. [[CrossRef](#)]
30. Wu, G.H.; Gao, L.H.; Zhang, Y.T.; Ning, C.Z.; Xie, E. Fracture attributes in reservoir-scale carbonate fault damage zones and implications for damage zone width and growth in the deep subsurface. *J. Struct. Geol.* **2019**, *118*, 181–193. [[CrossRef](#)]
31. Wan, X.G.; Wu, G.H.; Yang, P.F.; Gao, L.H. The seismic technique description of carbonate fault damage zone in Halahatang area, Tarim basin. *Oil Gas Geol.* **2016**, *37*, 785–791, (In Chinese with English abstract).
32. Gao, Z.Q.; Fan, T.L. Carbonate platform-margin architecture and its influence on Cambrian-Ordovician reef-shoal development, Tarim Basin, NW China. *Mar. Pet. Geol.* **2015**, *68*, 291–306. [[CrossRef](#)]
33. Zhao, K.Z.; Zhang, L.J.; Zheng, D.M.; Sun, C.H.; Dang, Q.N. A reserve calculation method for fracture-cavity carbonate reservoirs in Tarim Basin, NW China. *Pet. Explor. Dev.* **2015**, *42*, 277–282. [[CrossRef](#)]
34. Ni, X.F.; Shen, A.J.; Pan, W.Q.; Zhang, R.H.; Yu, H.F.; Dong, Y.; Zhu, Y.F.; Wang, C.F. Geological modeling of excellent fracture-vug carbonate reservoirs: A case study of the Ordovician in the northern slope of Tazhong palaeo-uplift and the southern area of Tabei slope, Tarim Basin, NW China. *Pet. Explor. Dev.* **2013**, *40*, 444–453. [[CrossRef](#)]

35. Viniestra, F.; Castillo-Tejero, C. Golden Lane fields, Veracruz, Mexico, in *Geology of giant petroleum fields. AAPG Mem.* **1970**, *14*, 309–325.
36. Howard, J.P.; Bogolepova, O.K.; Gubanov, A.P.; Gómez-Pérez, M. The petroleum potential of the Riphean–Vendian succession of southern East Siberia. *Geol. Soc. Lond. Spec. Publ.* **2012**, *366*, 177–198. [[CrossRef](#)]
37. Palmer, A.N. Origin and morphology of limestone caves. *Geol. Soc. Am. Bull.* **1991**, *103*, 1–21. [[CrossRef](#)]
38. Davies, G.R.; Smith, L.B. Structurally controlled hydrothermal dolomite reservoir facies: An overview. *AAPG Bull.* **2006**, *90*, 1641–1690. [[CrossRef](#)]
39. Cazarin, C.L.; Bezerra, F.H.R.; Borghic, L.; Santosd, R.V.; Favoretoc, J.; Brode, J.A.; Aulerf, A.S.; Srivastavab, N.K. The conduit-seal system of hypogene karst in Neoproterozoic carbonates in northeastern Brazil. *Mar. Pet. Geol.* **2019**, *101*, 90–107. [[CrossRef](#)]
40. Zhang, H.; Cai, Z.X.; Qi, L.X.; Yun, L. Diagenesis and origin of porosity formation of Upper Ordovician carbonate reservoir in northwestern Tazhong condensate field. *J. Nat. Gas Sci. Eng.* **2017**, *38*, 139–158. [[CrossRef](#)]
41. Croizé, D.; Renard, F.; Gratier, J.-P. Compaction and porosity reduction in carbonates: A review of observations, theory and experiments. *Adv. Geophys.* **2013**, *54*, 181–238.
42. Baud, P.; Rolland, A.; Heap, M.; Xu, T.; Nicolé, M.; Ferrand, T.; Reuschlé, T.; Toussaint, R.; Conil, N. Impact of stylolites on the mechanical strength of limestone. *Tectonophysics* **2016**, *690*, 4–20. [[CrossRef](#)]
43. Toussaint, R.; Aharonov, E.; Koehn, D.; Gratier, J.P.; Ebner, M.; Baud, P.; Rolland, A.; Renard, F. Stylolites: A review. *J. Struct. Geol.* **2018**, *114*, 163–195. [[CrossRef](#)]
44. Laubach, S.E.; Eichhubl, P.; Hargrove, P.; Ellis, M.A.; Hooker, J.N. Fault core and damage zone fracture attributes vary along strike owing to interaction of fracture growth, quartz accumulation, and differing sandstone composition. *J. Struct. Geol.* **2014**, *68*, 207–226. [[CrossRef](#)]
45. Pollard, D.D.; Aydin, A. Progress in understanding jointing over the past century. *Geol. Soc. Am. Bull.* **1998**, *100*, 1181–1204. [[CrossRef](#)]
46. Becker, S.P.; Eichhubl, P.; Laubach, S.E.; Reed, R.M.; Lander, R.H.; Bodnar, R.J. A 48 m.y. history of fracture opening, temperature, and fluid pressure: Cretaceous Travis Peak Formation, East Texas Basin. *GSA Bull.* **2010**, *122*, 1081–1093. [[CrossRef](#)]
47. Choquette, P.W.; Pray, L.C. Geologic nomenclature and classification of porosity in sedimentary carbonates. *AAPG Bull.* **1970**, *54*, 207–250.
48. Jia, L.Q.; Cai, C.F.; Jiang, L.; Zhang, K.; Li, H.X.; Zhang, W. Petrological and geochemical constraints on diagenesis and deep burial dissolution of the Ordovician carbonate reservoirs in the Tazhong area, Tarim Basin, NW China. *Mar. Pet. Geol.* **2016**, *78*, 271–290. [[CrossRef](#)]
49. Liu, W.; Huang, Q.Y.; Wang, K.; Shi, S.Y.; Jiang, H. Characteristics of hydrothermal activity in the Tarim Basin and its reworking effect on carbonate reservoirs. *Nat. Gas Ind. B* **2016**, *3*, 202–208. [[CrossRef](#)]
50. Wang, Z.Y.; Wu, L.; Zhang, Y.F.; Han, J.F.; Zhang, L.J. Study on category and forming environment of Upper Ordovician carbonate rock calcite cement in Tazhong district. *J. Earth Sci. Environ.* **2009**, *31*, 265–271. (In Chinese with English abstract).
51. Wu, G.H.; Yang, H.J.; He, S.; Cao, S.J.; Liu, X.; Jing, B. Effects of structural segmentation and faulting on carbonate reservoir properties: A case study from the Central Uplift of the Tarim Basin, China. *Mar. Petrol. Geol.* **2016**, *71*, 183–197. [[CrossRef](#)]
52. Weedman, S.D.; Brantley, S.L.; Shiraki, R.; Poulson, S.R. Diagenesis, compaction, and fluid chemistry modeling of a sandstone near a pressure seal: Lower Tuscaloosa Formation, Gulf Coast. *AAPG Bull.* **1996**, *80*, 1045–1064.
53. Franks, S.G.; Forester, R.W. Relationships among Secondary Porosity, Pore-Fluid Chemistry and Carbon Dioxide, Texas Gulf Coast. *AAPG Bull. Mem.* **1984**, *37*, 63–79.

